Discovery of protein- and DNA-imperceptible nanoparticle hard coating using gel-based reaction tuning

Kevin Welsher, Simon A. McManus, Chih-Hao Hsia, Shuhui Yin and Haw Yang

Department of Chemistry, Princeton University, Princeton, NJ 08544, United States

Supporting Information Placeholder

ABSTRACT: The seemingly inevitable protein corona appears as an insurmountable obstacle to a wider application of functional nanomaterials in biotechnology. The accumulation of serum proteins can block targeting functionalities and alter the *in vivo* fate of these nanomaterials. Here, we demonstrate a method to generate non-stick, robustly passivated functional nanoparticles using a tailored silica coating. We apply agarose gel electrophoresis to sensitively evaluate protein binding to nanoparticles with different surface chemistry. Using gel banding and retardation as a read-out for protein adsorption, we optimized the surface chemistry to yield a mixed charge surface which displayed remarkable binding resistance to a wide range of serum proteins and nucleic acids. The hard silica shell also protects the functional nanoparticle core in harsh environments (down to pH 1), while still showing the ability to be targeted for cellular uptake with little or no non-specific binding.

A major challenge in realizing the full potential of functional nanomaterials as sensors and diagnostics for biomedical applications is the control of their interaction with biological fluids. For example, in order to disperse a nanomaterial in biological media while maintaining the desired functionality (e.g. luminescence), the nanomaterial must be shielded from the potentially incapacitating elements in biological environments such as high salt concentration, extreme pH, and non-specific adsorption of biological macromolecules—the seemingly inevitable "protein corona."[1-4] In the past, efforts towards robust passivation have been largely focused on the use of hydrophilic polymers, such as polyethylene glycol (PEG)[5,6] or small molecule zwitterionic ligands.[7-12] For quantum dots (QDs), these methods using organic molecule based soft ligands typically rely on non-covalent, thiol-based interaction of the ligand with the nanoparticle's surface. As a result, even if the ligand itself is completely anti-fouling, the non-covalent nature of the interaction could lead to corruption of the passivation layer, particularly in bio-mimicking conditions.

Here, we report taking a different approach to this problem: We adopted a hard silica coating strategy, reasoning that the three dimensional covalent structure of silica could bestow long-term stability to the protective layer.[13-16] To tune the surface chemistry for biocompatibility, we apply a stringent test for protein adsorption based on agarose gel electrophoresis, which is frequently applied to study nanoparticle-protein interactions[17-19] and which has been shown to be able sensitive enough to resolve the interaction of a nanoparticle with a single protein.[20] Using this assay as a functional readout for surface chemistry optimization, we found that the resulting nanoparticles are surprisingly resistant to non-specific protein adsorption. It is generally believed that upon exposure to biological fluids, most if not all nanoparticles acquire a protein coating via non-specific adsorption. This protein coating, in turn, can block the desired function of the nanoparticle surface and completely change its *in vivo* fate.[21-24] The method described below provides one fine example that it is possible to control a nanoparticle surface such that it is protein corona resistant, at least at an assay level as sensitive as gel electrophoresis or dynamic light scattering (DLS). The optimized nanoparticle construct consists of a mixed charge silica-coated surface that resists binding to common serum proteins, while maintaining luminescence of the encapsulated nanoparticle in acidic environments (down to pH 1). These traits are achieved all while maintaining the ability to functionalize the nanoparticle surface through simple amine chemistry, imparting a tremendous amount of potential applications to these robust, non-stick particles.

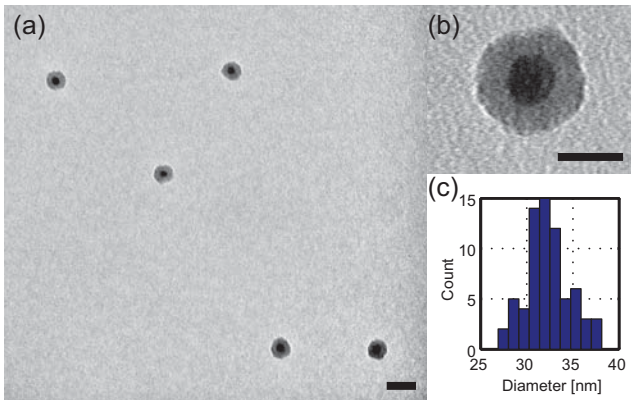

Figure 1. TEM of monodisperse gQD@SiO_2 particles. The dark center corresponds to the alloyed CdSe/CdS structure, while the light outer shell is due to the silica coating. Scale bar represent (a) 50 nm and (b) 20 nm. (c) Size distribution histogram of gQD@SiO_2 particles (n = 69), yielding a diameter of 32.3 ± 2.5 nm.

We utilized non-blinking giant quantum dots (gQDs, Figure S1-S3) as a model system for designing silica-coated nanoparticles because their luminescence provided a direct readout of successful and robust passivation. Furthermore, gQDs are ideal for both *in vivo* imaging and single-molecule tracking applications as they are both non-blinking and non-bleaching. These gQDs were synthesized according to previously reported protocols[25,26] and were found to display a minimal amount of blinking behavior (Fig. S2). To provide the hard coating and to serve as a flexible platform for surface tuning, silica shell growth was performed using tetraethoxyorthosilicate (TEOS) in a reverse-microemulsion.[13] For a simple, non-substituted coating, the reaction was allowed to proceed for 5 hours at room temperature to yield uniformly coated and water soluble gQDs (gQD@SiO_2, Figure 1). Importantly, the gQD@SiO_2 particles showed impressive maintenance of quantum

yield (~18%, down from ~22% in hexanes) during the transition from organic to aqueous environment. Unfortunately, this simple silica coating was not sufficient for biological applications, as the resulting particles were not stable in buffered solution. However, as discussed below, the electrostatic manipulation of the coating via the addition of charged silane-reactive species in the microemulsion-assisted silica encapsulation process resolves this issue.

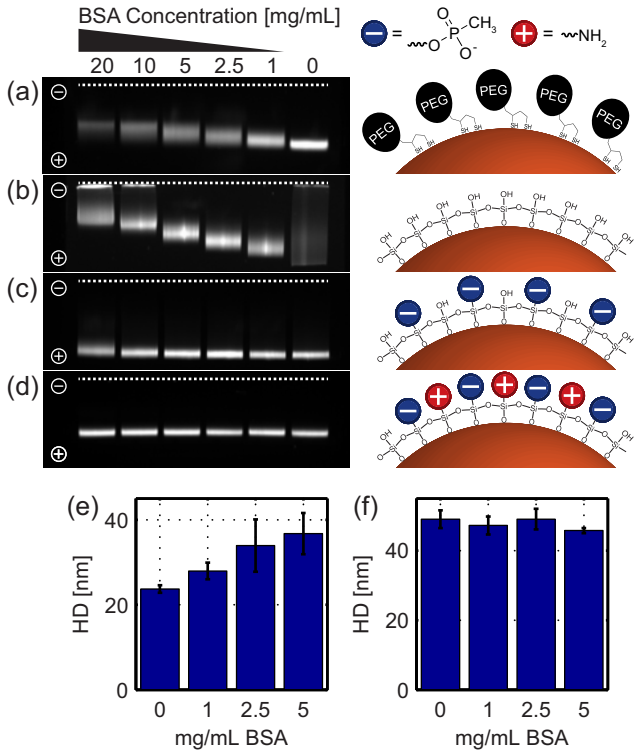

Figure 2. Tuning the protein binding of gQD@SiO_2 particles. Nanoparticles were subjected to increasing concentrations of BSA to determine the amount of protein adsorption to the nanoparticle surface. (a) gQD-DHLA-PEG shows reduced electrophoretic mobility as a function of BSA concentration. (b) Simple silica coating of the gQD nanoparticles shows more severe effects of protein binding relative to the gQD-DHLA-PEG particles shown in (a), as well as smearing in the PBS only control, indicating buffer instability. (c) The addition of an optimized amount of THSPMP (21 μmol) to the reaction mixture results in drastically reduced protein binding, with only a small change in electrophoretic mobility observed at the highest BSA concentration tested (20 mg/mL). (d) Addition of amine groups on the surface via APTES (4.3 μmol, 31.5 μmol THSPMP) results in no detectable BSA binding. (e) DLS of gQD-DHLA-PEG particles incubated with increasing amounts of BSA, showing an increase in hydrodynamic diameter as a function of BSA concentration (HD = hydrodynamic diameter). (f) DLS of optimized gQD@SiO_2 particles versus BSA concentration, showing no change in hydrodynamic diameter as a function of BSA concentration.

Next we demonstrate a simple yet sensitive assay based on gel electrophoresis to evaluate the formation of the protein corona. Agarose gel electrophoresis is an ideal tool to evaluate the protein corona, as it has been shown to be able to detect the presence of a single protein on the surface of a quantum dot.[27] The sensitivity of our assay was obtained by optimizing gel running conditions to allow distinction between free gQD@SiO_2 particles and gQD@SiO_2 bound to one or more proteins. A critical factor was the use of very low concentration agarose gels (0.2%) to allow the relatively large gQD@SiO_2 to migrate a sufficiently long distance. As a baseline, we tested the tendency for protein adsorption on the surface of gQDs functionalized with the most widely implemented quantum dot passivation method: surface-binding of dihydrolipoic acid (DHLA) moieties terminated with polyethylene glycol.[28,29] Protein adsorption was evaluated by incubating the particles with increasing amounts of bovine serum albumin (BSA), a protein that binds with high affinity to a wide range of nanoparticles.[1] After incubation, the samples were analyzed via agarose gel electrophoresis to detect changes in both the size and surface charge of the nanoparticles (Figure 2a). The control lane, where gQD-DHLA-PEG was incubated in PBS only, showed a tight band, indicating uniform particle size and stability in the buffer environment. In increasing BSA concentrations, however, the gQD-DHLA-PEG band decreased in mobility, indicating an increase in size or reduction in the surface charge of the construct. This shift was concentration dependent, approaching saturation at 20 mg/mL BSA. This indicated that the gQD's surface was coated with BSA, either by surrounding the DHLA-PEG ligand layer or actively displacing those ligands. As an additional control, this readout was also applied to 20 nm carboxy-modified polystyrene particles, which showed similar band shifts as a function of BSA concentration (Figure S4). The non-functionalized gQD@SiO_2 particles under the gel-based assay also showed severe binding of the test protein BSA (Figure 2b). This is consistent with previous literature reports which show that silica nanoparticles display a proclivity for protein corona formation.[30-32] The control lane shows a smeared band, indicating that the particles were not stable in a buffered environment. The addition of 1 mg/mL BSA both tightened the band and retarded its mobility. In this case, the binding of BSA to the surface likely imparted buffer stability and prevented particle-particle aggregation.[30] Increasing amounts of BSA led to decreasing electrophoretic mobility, with high BSA concentrations (above 10 mg/mL) eventually leading to particle aggregation, evidenced by particles not leaving the well. With the goal of reducing protein adsorption, the BSA titration described above was used as a functional readout to determine the protein affinity of a given gQD@SiO_2 formulation. Using this readout as a guide, the surface chemistry of the gQD@SiO_2 particles was tuned to achieve differential protein binding. Surface charge was tuned via the addition of 3-(trihydroxysilyl)propyl methylphosphonate (negative charge, THSPMP) and (3-aminopropyl)triethoxysilane (positive charge, APTES). Addition of a small amount of THSPMP to the reaction mixture yielded particles which were buffer stable, as evidenced by the reduced smearing and increased band tightness in the gel (Figure S5b). As the amount of THSPMP added to the reaction mixture was increased, the affinity for BSA approached a minimum at 21.0 μmol THSPMP, showing a slight shift in mobility only at the highest (20 mg/mL) BSA concentration (Figure 2c, Figure S5c). Further addition of THSPMP actually led to increased protein binding (Figure S5d-e). Surprisingly, at the optimized THSPMP condition, the addition of amine to the surface of the gQD@SiO_2 particle acts to completely eliminate this affinity for protein adsorption, with the particle showing no change in electrophoretic mobility even at 20 mg/mL BSA (Figure 2d, Figure S5f-i). It should be noted that amine on its own was insufficient for particle functionalization. Particles which were synthesized with APTES in the absence of THSPMP were not water soluble, while the addition of a small amount of methylphosphonate yielded particles which were water soluble, buffer stable, and resistant to protein adsorption (Figure S8).

These gel-assay results were corroborated by those from dynamic light scattering (DLS), which has been a workhorse in the protein

corona field. The gQD-DHLA-PEG samples showed a steady increase in the hydrodynamic diameter as a function of BSA concentration (Figure 2e). The DLS scans on the optimized gQD@SiO_2 particles incubated with varying levels of BSA showed no significant change in the hydrodynamic diameter, confirming that protein binding is indeed minimized (Figure 2f).

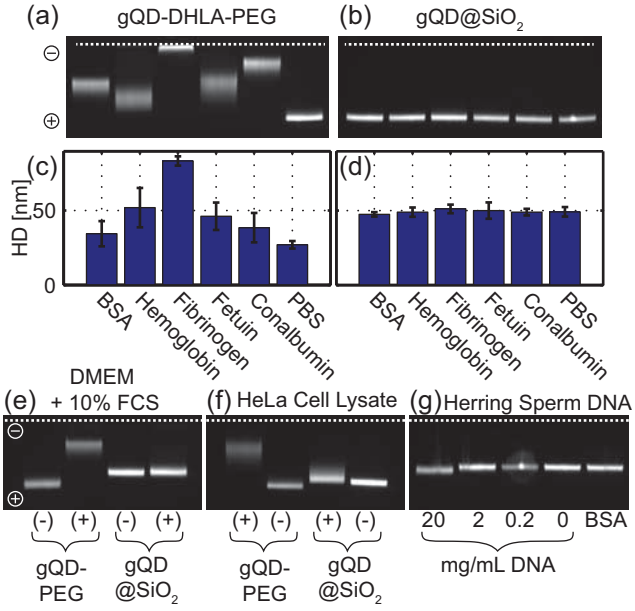

Figure 3. Binding of various proteins to gQD conjugates. (a) Agarose gel of gQD-DHLA-PEG particles incubated with a variety of serum proteins (as labeled in c), showing a wide range of effects on the electrophoretic mobility. (b) Agarose gel of optimized gQD@SiO_2 particles, showing no change in electrophoretic mobility with any of the serum proteins tested. (c) DLS on gQD-DHLA-PEG after incubation with serum proteins, showing increased hydrodynamic diameter with all proteins tested, corroborating the agarose gel results (HD = hydrodynamic diameter). (d) DLS on optimized gQD@SiO_2 particles, showing no significant change in size after protein incubation. (e) Agarose gel showing protein binding in the presence of cell media. gQD-DHLA-PEG displays a large change in mobility, while gQD@SiO_2 particles remain unaffected. (f) Electrophoretic mobility in the presence of HeLa cell lysate, where gQD-DHLA-PEG shows a drastic shift, while the gQD@SiO_2 particles show only a small shift and smearing. (g) Binding analysis of herring sperm DNA to the optimized gQD@SiO_2 formulation, showing a small increasing in particle mobility only at the highest nucleic acid concentration.

Remarkably, despite using BSA as a test protein, the optimized gQD@SiO_2 particles were found to resist a wide range of biological molecules. Figure 3a-d shows the gel electrophoresis and DLS results for both gQD-DHLA-PEG and gQD@SiO_2 particles when incubated with a variety of different serum proteins, including hemoglobin, fibrinogen, fetuin and conalbumin. The gQD-DHLA-PEG nanoparticles showed binding to all of these proteins at a concentration of 1 mg/mL, with fibrinogen causing the most marked change in both electrophoretic mobility and hydrodynamic diameter. The optimized gQD@SiO_2 conjugate, on the other hand, showed no evidence of protein binding, either in the gel assay or DLS. This indicates a remarkable resistance to protein adsorption has been provided by the optimized silica surface.

These formulations were then tested against cell media with 10% fetal calf serum (Figure 3e), HeLa cell lysate (Figure 3f) and herring sperm DNA (hsDNA, Figure 3g). The gQD@SiO_2 particles showed excellent resistance to the cell media, while some smearing was observed in the case of the cell lysate. When compared to gQD-DHLA-PEG however, the mobility was much less retarded, indicating that gQD@SiO_2 bound to much fewer molecules in this complex mixture. The hsDNA tests showed that there is some binding at 20 mg/mL nucleic acid concentration to the optimized gQD@SiO_2 formulation, evidenced by a small increase in electrophoretic mobility, though it should be noted that this far exceeds the expected nucleic acid concentration in the cell.[33] This was markedly different from the gQD-DHLA-PEG particles, which showed a decrease in electrophoretic mobility in the presence of even small amounts of nucleic acids (Figure S9).

The method for generating a "non-stick" surface for functional nanoparticles described above is not restricted to gQDs, but can be easily extended to other nanoparticle systems. The same resistance to BSA adsorption was observed when the gQD particles were replaced with commercial Qdot 605 from Life Technologies (Figure S11) and oleylamine coated gold nanoparticles (Figure S12). This method thus has the potential to be applied to any functional nanoparticle, provided that it is soluble in organic solvent.

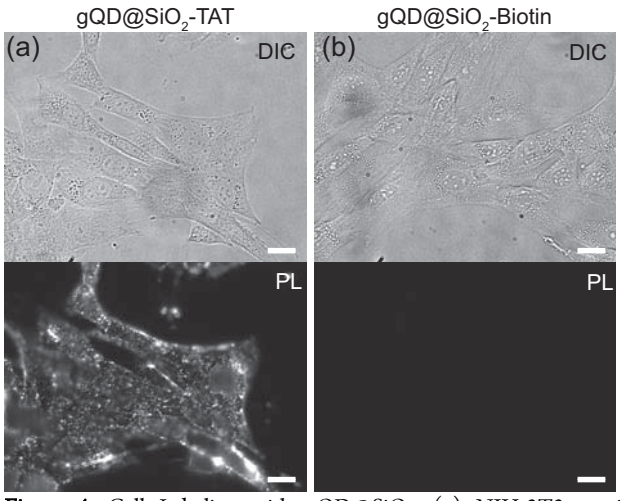

Figure 4. Cell Labeling with gQD@SiO_2. (a) NIH-3T3 murine fibroblast cells were incubated with gQD@SiO_2-Tat particles, showing a high degree of binding and uptake. (b) Control particles without Tat conjugation showed no sign of binding under the same conditions. Scale bars represent 20 μm.

Critical to any downstream application of functional nanoparticles is the ability to covalently attach proteins or targeting molecules to impart biological function. On its own, the ability to inhibit protein binding in a biological fluid is important, but not if the end result is a completely inert nanoparticle. Importantly, these gQD@SiO_2 particles still maintain the ability to be further functionalized, owing to the presence of amine groups on the particle surface. As a demonstration, gQD@SiO_2 particles were functionalized with Tat, a cationic peptide derived from HIV, also known as a cell penetrating peptide.[34,35] The gQD@SiO2 nanoparticles were functionalized with the HIV1-Tat peptide first by adding NHS-PEG-biotin to the surface, followed by streptavidin binding. The streptavidin coated particles were then incubated with Tat-biotin. The addition of the peptide to the gQD@SiO_2 surface allows for high binding and uptake of nanoparticles when incubated with NIH-3T3 fibroblasts (Figure 4a, Figures S14-S17). Critically, there is no detectable binding or uptake of gQD@SiO_2 particles

without Tat (Figure 4b, Figure S16). These particles were also able to targeted to specific cell surface receptors using ligands such as human epidermal growth factor (EGF)[36] with no detectable non-specific binding (Figure S18). Finally, these particles display remarkable long term stability in water (up to 5 months, Figure S19), as well as exhibiting resistance to acid corrosion, even down to pH 1 (Figure S20). The unique combination of the biologically non-interacting, robust coating with the non-blinking gQD core promises the realization of real-time 3D single particle tracking[37,38] or 3D multi-resolution microscopy[39] in harsh environments. A representative real-time 3D single particle trajectory of a non-blinking gQD@SiO_2 particle is shown in Figure S21.

We propose that the method described above is generally applicable to tuning the protein adsorption of nanoparticle constructs. Instead of trying to predict the best monofunctional ligand, one can instead read out the concentration dependent protein binding and monitor the changes as a function of surface chemistry modifications. Following this route, a minimum can be found in the adsorption of the chosen biologic. Here, we have applied this method to generate robust, water-soluble functional nanoparticles with extremely low affinity for biological fluids and resistance to harsh environments. The optimized gQD@SiO_2 particles described herein represent the first non-blinking, non-bleaching, non-stick and extreme acid tolerant nanoparticle construct. The flexibility of this passivation procedure allows it to be further extended to commercially available functional nanoparticles, such as conventional quantum dots and gold nanoparticles. The ability to passivate any particle will make this a powerful method for developing potentially long-circulating non-stick particles for a variety of drug delivery and targeted *in vivo* imaging applications, especially given the robust nature of the silica shell, which has been shown to persist for weeks to months in the in vivo environment.[40,41] Critically, as demonstrated here, the optimized non-stick silica shell does not preclude further functionalization, allowing these biologically non-interacting nanoparticles to interact specifically only with a desired target.

ASSOCIATED CONTENT

Supporting Information

Materials and methods, gQD@SiO_2 synthesis, application of optimized coating to other nanoparticles. This material is available free of charge via the Internet at http://pubs.acs.org.

AUTHOR INFORMATION

Corresponding Author

hawyang@princeton.edu

Notes

The authors declare no competing financial interests.

ACKNOWLEDGMENT

This work was supported by the Department of Energy (DE-SC0006838) and Princeton University. We would also like to thank the Imaging and Analysis Center of Princeton University for assisting with TEM measurements.

REFERENCES

(1) Walkey, C. D.; Chan, W. C. W. *Chem. Soc. Rev.* **2012**, *41*, 2780.
(2) Monopoli, M. P.; Aberg, C.; Salvati, A.; Dawson, K. A. *Nat. Nanotechnol.* **2012**, *7*, 779.
(3) Lundqvist, M.; Stigler, J.; Elia, G.; Lynch, I.; Cedervall, T.; Dawson, K. A. *Proc. Natl. Acad. Sci. U. S. A.* **2008**, *105*, 14265.
(4) Cedervall, T.; Lynch, I.; Lindman, S.; Berggard, T.; Thulin, E.; Nilsson, H.; Dawson, K. A.; Linse, S. *Proc. Natl. Acad. Sci. U. S. A.* **2007**, *104*, 2050.
(5) Owens Iii, D. E.; Peppas, N. A. *Int. J. Pharm.* **2006**, *307*, 93.
(6) Gref, R.; Lück, M.; Quellec, P.; Marchand, M.; Dellacherie, E.; Harnisch, S.; Blunk, T.; Müller, R. H. *Colloids Surf., B* **2000**, *18*, 301.
(7) Zhan, N.; Palui, G.; Safi, M.; Ji, X.; Mattoussi, H. *J. Am. Chem. Soc.* **2013**, *135*, 13786.
(8) Zhan, N.; Palui, G.; Grise, H.; Tang, H.; Alabugin, I.; Mattoussi, H. *ACS Appl. Mater. Interfaces* **2013**, *5*, 2861.
(9) Estephan, Z. G.; Hariri, H. H.; Schlenoff, J. B. *Langmuir* **2013**, *29*, 2572.
(10) Estephan, Z. G.; Jaber, J. A.; Schlenoff, J. B. *Langmuir* **2010**, *26*, 16884.
(11) Moyano, D. F.; Saha, K.; Prakash, G.; Yan, B.; Kong, H.; Yazdani, M.; Rotello, V. M. *ACS Nano* **2014**, *8*, 6748.
(12) Chour, W.; Hsia, C.-H.; Knowles, R. R.; Yang, H. *Submitted* **2014**.
(13) Han, Y.; Jiang, J.; Lee, S. S.; Ying, J. Y. *Langmuir* **2008**, *24*, 5842.
(14) Selvan, S. T.; Patra, P. K.; Ang, C. Y.; Ying, J. Y. *Angew. Chem., Int. Ed.* **2007**, *46*, 2448.
(15) Zhelev, Z.; Ohba, H.; Bakalova, R. *J. Am. Chem. Soc.* **2006**, *128*, 6324.
(16) Gerion, D.; Pinaud, F.; Williams, S. C.; Parak, W. J.; Zanchet, D.; Weiss, S.; Alivisatos, A. P. *J. Phys. Chem. B* **2001**, *105*, 8861.
(17) Aubin-Tam, M.-E.; Hamad-Schifferli, K. *Langmuir* **2005**, *21*, 12080.
(18) Pinaud, F.; King, D.; Moore, H.-P.; Weiss, S. *J. Am. Chem. Soc.* **2004**, *126*, 6115.
(19) Pons, T.; Uyeda, H. T.; Medintz, I. L.; Mattoussi, H. *The Journal of Physical Chemistry B* **2006**, *110*, 20308.
(20) Howarth, M.; Liu, W.; Puthenveetil, S.; Zheng, Y.; Marshall, L. F.; Schmidt, M. M.; Wittrup, K. D.; Bawendi, M. G.; Ting, A. Y. *Nat Meth* **2008**, *5*, 397.
(21) Tenzer, S.; Docter, D.; Kuharev, J.; Musyanovych, A.; Fetz, V.; Hecht, R.; Schlenk, F.; Fischer, D.; Kiouptsi, K.; Reinhardt, C.; Landfester, K.; Schild, H.; Maskos, M.; Knauer, S. K.; Stauber, R. H. *Nat. Nanotechnol.* **2013**, *8*, 772.
(22) Mirshafiee, V.; Mahmoudi, M.; Lou, K.; Cheng, J.; Kraft, M. L. *Chem. Commun.* **2013**, *49*, 2557.
(23) Lesniak, A.; Fenaroli, F.; Monopoli, M. R.; Aberg, C.; Dawson, K. A.; Salvati, A. *ACS Nano* **2012**, *6*, 5845.
(24) Walkey, C. D.; Olsen, J. B.; Song, F.; Liu, R.; Guo, H.; Olsen, D. W. H.; Cohen, Y.; Emili, A.; Chan, W. C. W. *ACS Nano* **2014**, *8*, 2439.
(25) Ghosh, Y.; Mangum, B. D.; Casson, J. L.; Williams, D. J.; Htoon, H.; Hollingsworth, J. A. *J. Am. Chem. Soc.* **2012**, *134*, 9634.
(26) Chen, Y.; Vela, J.; Htoon, H.; Casson, J. L.; Werder, D. J.; Bussian, D. A.; Klimov, V. I.; Hollingsworth, J. A. *J. Am. Chem. Soc.* **2008**, *130*, 5026.
(27) Howarth, M.; Liu, W. H.; Puthenveetil, S.; Zheng, Y.; Marshall, L. F.; Schmidt, M. M.; Wittrup, K. D.; Bawendi, M. G.; Ting, A. Y. *Nat. Methods* **2008**, *5*, 397.
(28) Susumu, K.; Mei, B. C.; Mattoussi, H. *Nat. Protoc.* **2009**, *4*, 424.
(29) Clapp, A. R.; Goldman, E. R.; Mattoussi, H. *Nat. Protoc.* **2006**, *1*, 1258.
(30) Monopoli, M. P.; Walczyk, D.; Campbell, A.; Elia, G.; Lynch, I.; Bombelli, F. B.; Dawson, K. A. *J. Am. Chem. Soc.* **2011**, *133*, 2525.
(31) Tenzer, S.; Docter, D.; Rosfa, S.; Wlodarski, A.; Kuharev, J.; Rekik, A.; Knauer, S. K.; Bantz, C.; Nawroth, T.; Bier, C.; Sirirattanapan, J.; Mann, W.; Treuel, L.; Zellner, R.; Maskos, M.; Schild, H.; Stauber, R. H. *ACS Nano* **2011**, *5*, 7155.
(32) Salvati, A.; Pitek, A. S.; Monopoli, M. P.; Prapainop, K.; Bombelli, F. B.; Hristov, D. R.; Kelly, P. M.; Aberg, C.; Mahon, E.; Dawson, K. A. *Nat Nano* **2013**, *8*, 137.
(33) Human Genome Sequencing, C. *Nature* **2004**, *431*, 931.
(34) Tyagi, M.; Rusnati, M.; Presta, M.; Giacca, M. *J. Biol. Chem.* **2001**, *276*, 3254.
(35) Vives, E.; Brodin, P.; Lebleu, B. *J. Biol. Chem.* **1997**, *272*, 16010.
(36) Yarden, Y.; Sliwkowski, M. X. *Nat. Rev. Mol. Cell Biol.* **2001**, *2*, 127.
(37) Cang, H.; Xu, C. S.; Montiel, D.; Yang, H. *Opt. Lett.* **2007**, *32*, 2729.
(38) Cang, H.; Wong, C. M.; Xu, C. S.; Rizvi, A. H.; Yang, H. *Appl. Phys. Lett.* **2006**, *88*, 223901.
(39) Welsher, K.; Yang, H. *Nat. Nanotechnol.* **2014**, *9*, 198.
(40) Cho, M.; Cho, W.-S.; Choi, M.; Kim, S. J.; Han, B. S.; Kim, S. H.; Kim, H. O.; Sheen, Y. Y.; Jeong, J. *Toxicol. Lett.* **2009**, *189*, 177.
(41) Xie, G.; Sun, J.; Zhong, G.; Shi, L.; Zhang, D. *Arch. Toxicol.* **2010**, *84*, 183.

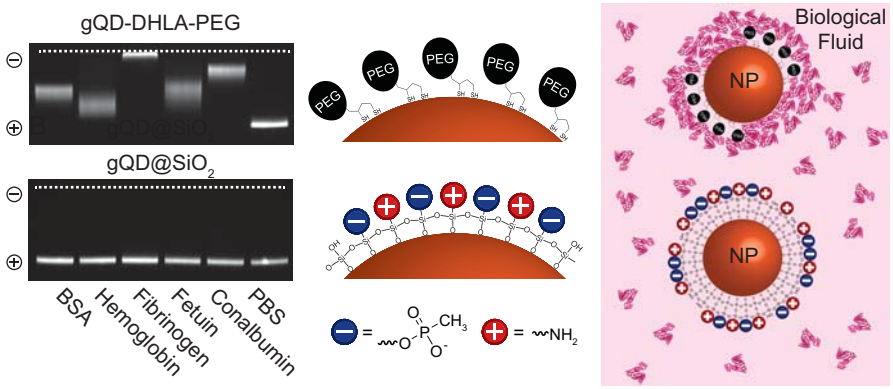
gQD-DHLA-PEG
gQD@SiO2
BSA
Hemoglobin
Fibrinogen
Fetuin
Conalbumin
PBS
PEG
Biological Fluid
NP
NP